

Suppression of the Aharonov-Bohm effect in hexagonal quantum rings

A. BALLESTER¹, C. SEGARRA¹, A. BERTONI² and J. PLANELLES¹

¹ *Departament de Química Física i Analítica, Universitat Jaume I - Castelló de la Plana, Spain*

² *Centro S3, CNR-Istituto Nanoscienze - Via Campi 213/A, Modena, Italy*

PACS 75.75.-c – Magnetic properties of nanostructures

PACS 73.21.Hb – Quantum wires

PACS 73.21.La – Quantum dots

PACS 03.65.-w – Quantum mechanics

Abstract – Few-electron states of AlAs-GaAs-AlAs hexagonal quantum rings pierced by an axial magnetic field are computed through full configuration interaction calculations. The quantum ring is in the low-density regime, populated with $N = 1$ up to $N = 7$ electrons. Similar to circular rings, the energy spectra of the hexagonal ones reflect an integer and fractional Aharonov-Bohm regular oscillation pattern for $N = 1$ and $N = 2, 3$, respectively. Deviations from the regular fractional period with increasing electron density become apparent for larger N . Remarkably, for $N = 6$ the Aharonov-Bohm effect is completely suppressed. This is a unique symmetry-related feature of hexagonal rings that only can emerge in the low-density regime.

Introduction. – Most III-V nanowires with a diameter less than about 400 nm have a very neat hexagonal section even after a few overcoating processes. [1–6] These core-multishell nanowires have an unconstrained longitudinal direction and different material composition along the orthogonal plane (radial direction), that eventually bound carriers on a prismatic tube surrounding the central core. With a proper material modulation along the growth axis, or just by cutting them, a strong confinement of carriers in the longitudinal direction can be introduced [7–10] leading to a hexagonal flat quantum ring (QR) where the free carriers are confined on a square-well type potential in the radial direction. [11] These flat polygonal structures are much less studied than their circular counterparts, where evidences of the Aharonov-Bohm (AB) effect have given rise to a decade of intensive research. [12–18] One then wonders what differences can be expected from the different confinement symmetry of hexagonal rings.

In a recent paper [19] we presented a theoretical study of correlated multi-electron states of hexagonal semiconductor rings populated with $N = 1$ up to $N = 7$ electrons and found that charges get more localized in the corners as the number of electrons increases up to $N = 6$, where we found a maximum of localization. The result evidences

the deficiency of a picture based on orbitals delocalized on the whole ring, i.e. electron correlation becomes crucial. In this Letter we investigate the response of this N -electron system to an external axial magnetic field which brings AB physics into play. Specifically, we focus on the different response in comparison to circular QRs.

It is well known that an increase in the strength of an externally applied axial magnetic field in a circular QR leads to oscillations of the ground state energy. The period and amplitude of the oscillations depends on the electron population and it is referred to as fractional AB effect. [20] The first unambiguous experimental evidence of this effect may be traced back to the work by Keyser. [21] Soon after, Emperador et al. [22] related this fractional response to a low kinetic energy and a phenomenon of electronic localization. Full configuration interaction (FCI) calculations by Niemelä et al. [23] of QRs populated up to four electrons revealed the crucial role of electron-electron interaction on the decrease of the period and amplitude of the ground state energy and its fractional character. Liu et al. [24] extended the FCI calculation to QRs populated with $N = 5$ and $N = 6$ electrons as a function of the magnetic field and the QR radius, thus yielding a phase diagram with a rich variety of ground states. The fractional character

of the AB effect was though fully explored earlier using the empirical Hubbard model, [25] and it was concluded that fractional AB oscillations arise for small values of the factor $\alpha = Nt/(UL)$, where N is the number of electrons in the QR, t is the tunnelling integral, U the repulsion one and L the number of sites along the QR where the single-particle functions are located. For α to be small, the ratio between the one-electron integral t and the two-electron integral U must be small, i.e., a low kinetic energy and a strong electron-electron interaction is required. Also, since α is proportional to N , a low-density regime is needed. Additionally, L introduces the possible role of symmetry lowering: the larger L the sooner the Hubbard model reaches the fractional AB regime. But no other symmetry-related effect is reported.

In this work, we consider the same AlAs-GaAs-AlAs hexagonal QR studied in ref. [19], where all physical parameters, namely effective masses, conduction-band offset and dielectric constant can be found. We carry out calculations for $N = 2$ up to $N = 7$ interacting electrons in the low-density regime. We find that the low-energy spectrum of the hexagonal QR resembles that of circular ones. Like in circular QRs, the energy spectra of the hexagonal QRs analyzed here reflect an integer and regular AB oscillation pattern for $N = 1$, a fractional, also regular, AB oscillation pattern for $N = 2$ and $N = 3$, and deviations from the regular period with the increasing electron density. Specifically, $N = 4$ and $N = 5$ have not regular oscillation amplitude patterns, while $N = 7$ shows already an integer period, like that of $N = 1$. The most intriguing result is found for $N = 6$ electrons, where AB effect is completely suppressed, which translates into zero magnetization. We show this is a peculiar symmetry-related response of the $N = 6$ system in hexagonal QRs that only can emerge in the low-density regime.

Theory. – We perform an exact diagonalization of the multi-particle Schrödinger equation via a FCI procedure. As a first step, the single-particle orbitals ϕ_i and energies ϵ_i of the conduction band are computed through a real-space numerical solution of the eigenvalue equation of the effective-mass Hamiltonian,

$$h = \frac{1}{2}(\mathbf{p} + \mathbf{A}) \frac{1}{m^*(\mathbf{r})} (\mathbf{p} + \mathbf{A}) + V(\mathbf{r}) \quad (1)$$

where \mathbf{r} is the 2D coordinate on the hexagonal domain, $m^*(\mathbf{r})$ is the isotropic material-dependent effective mass of electrons, \mathbf{A} is the magnetic vector potential, and $V(\mathbf{r})$ is the confining potential, represented schematically in the inset of fig. 1. This equation is numerically integrated using the finite-elements method on a regular triangular mesh with hexagonal elements. The grid reproduces the symmetry of the system thus avoiding numerical artifacts originated by discretization asymmetries of the six domain boundaries, as would be the case, e.g., using a rectangular grid. Unless otherwise indicated, the

employed geometry is a regular hexagon domain with edges 66.5 nm long including a GaAs well 6.8 nm wide with uniform thickness all around the 37.3 nm AlAs core. The GaAs well is covered by a 13.5 nm AlAs capping layer (see inset in fig. 1).

Finally we diagonalize the multi-particle Hamiltonian

$$H = \sum_{i\sigma} \epsilon_i e_{i\sigma}^\dagger e_{i\sigma} + \frac{1}{2} \sum_{ijkl} \sum_{\sigma\sigma'} U_{ijkl} e_{i\sigma}^\dagger e_{j\sigma'}^\dagger e_{k\sigma'} e_{l\sigma} \quad (2)$$

where $e_{i\sigma}$ ($e_{i\sigma}^\dagger$) is the annihilation (creation) operator for an electron in the orbital state i and with spin σ . For all the calculations we use 24 spin-orbital single-particle states, giving $\binom{24}{N}$ Slater determinants, with N being the number of electrons.

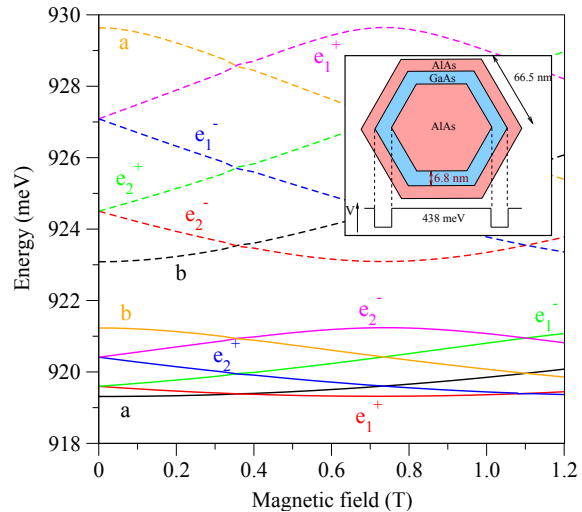


Fig. 1: Orbital energies vs. magnetic field, labelled according to the C_6 symmetry group. Two well-separated shells composed by 6 orbitals can be identified, with a 2 meV energy gap between them. Inset: Schematics of the system. The GaAs ring is wrapped around an hexagonal AlAs core and capped by an additional AlAs shell. The free electrons are confined in the GaAs region.

Results and discussion. – In fig. 1 we show the low-lying part of the single-electron energy spectrum as a function of the magnetic field. Orbitals are labelled according to the C_6 symmetry group. Well-separated with a 2 meV energy gap between them, we can identify two shells each composed by 6 orbitals. Namely, two groups of orbitals well separated in energy, having the same degeneracy pattern. The result, quite different from that of a circular QR, originates from the symmetry lowering when going from circular to hexagonal shape. In the first case we have an infinite number of irreducible representations (irreps) which associated orbitals can cross. By contrast, the hexagonal ring has only six irreps, so that anticrossings between orbitals with the same

symmetry appear. This opens a gap between the shells. The states cross with increasing field only within the shell where states have different symmetry (see fig. 1). As a consequence of the shell splitting, we find that in a wide range of the low-lying N -electron states only the lowest 6 orbitals (spin-independent real space wave functions) have significant population.

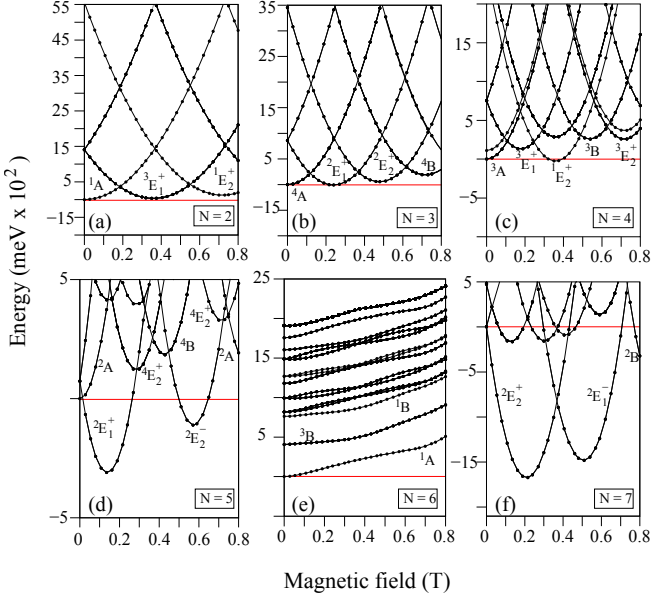


Fig. 2: Energy of low-lying few-electron states, labelled according to the C_6 symmetry group and spin multiplicity, vs. the magnetic field. The six panels show the cases of $N = 2$ to $N = 7$ electrons, as indicated. Zero energy, indicated by the straight reference line, corresponds to the ground state energy without magnetic field.

In fig. 2 we summarize the behaviour of the energy of lowest-lying few-electron states vs. the magnetic field. The represented energies are relative to the N -electron ground state energy in the absence of magnetic field (horizontal red line). The few-electron states are labelled according to the C_6 symmetry group and spin multiplicity of states. Figure 3 displays the corresponding magnetization in meV/T. We can see that for $N = 2$ and $N = 3$ a perfect fractional AB is observed. Thus, fig. 3 reveals that for $N = 2$ the AB period is halved as compared to the $N = 1$ case. Likewise, for $N = 3$ it is one third. Deviations of the regular fractional period become apparent for larger N . For $N = 4$ and especially for $N = 5$ the oscillation amplitude pattern is far from regular, and the $N = 7$ case already shows an integer period. The observed behaviour is consistent with the previous calculations on QRs. [22–25] In particular, the behaviour vs. N is consistent with an increasing α factor that prevents the fractional behaviour of the AB oscillations. [25]

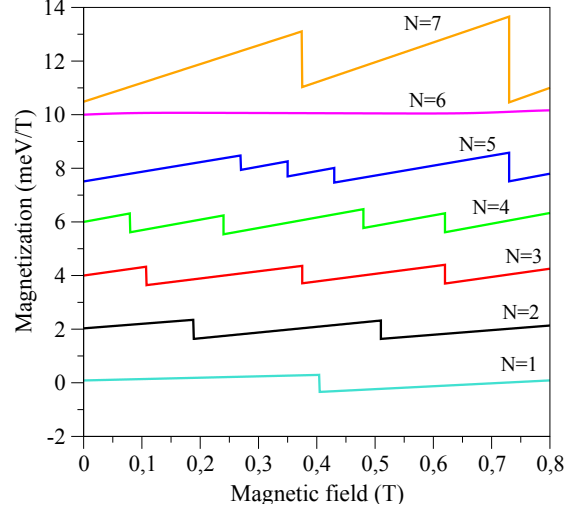


Fig. 3: Magnetization of the N -electron hexagonal QR vs. the applied magnetic field, for $N = 1$ (bottom) up to $N = 7$ (top). For the sake of clarity, the different magnetization profiles have been offset by 2 meV/T.

The most striking result in figs. 2 and 3 is found for $N = 6$. In this case a complete suppression of the AB oscillation that turns into a completely flat magnetization profile occurs.

In order to understand the peculiar behaviour of the $N = 6$ system, we repeated the set of FCI calculations but introducing a scaling factor f that multiplies the electron-electron interaction integrals. For $f = 0$ we obtain the non-interacting particle spectrum with a crossing, at about 1/2 of flux, of two different configurations, $a^2(e_1^+)^2(e_1^-)^2$ and $(e_1^+)^2a^2(e_2^+)^2$, corresponding to two different states 1A with the same total symmetry and total spin (see panel (a) in fig. 4). The first configuration is the lowest-lying one at $B = 0$ while the second represents a highly excited configuration at this magnetic field. The two configurations are essentially exchanged at about one unit of flux. When the electron-electron repulsion is included the string of symmetry-labels of the orbitals cannot be used as good quantum numbers, since the configuration interaction takes place. Then, only the total symmetry and total spin are good labels. However we can still identify these configurations as dominant, with a large contribution in the case of small f factors. In the presence of Coulomb interactions, the two 1A states having these leading configurations anticross, the anticrossing being larger as electron-electron interaction increases (see panels (b), (c) and (d) in fig. 4).

To further assess the role of the regime of density, we carried out calculations for an hexagonal QR three times smaller than the above sample. Simulations of magnetizations are reported in fig. 5. In this case, we can

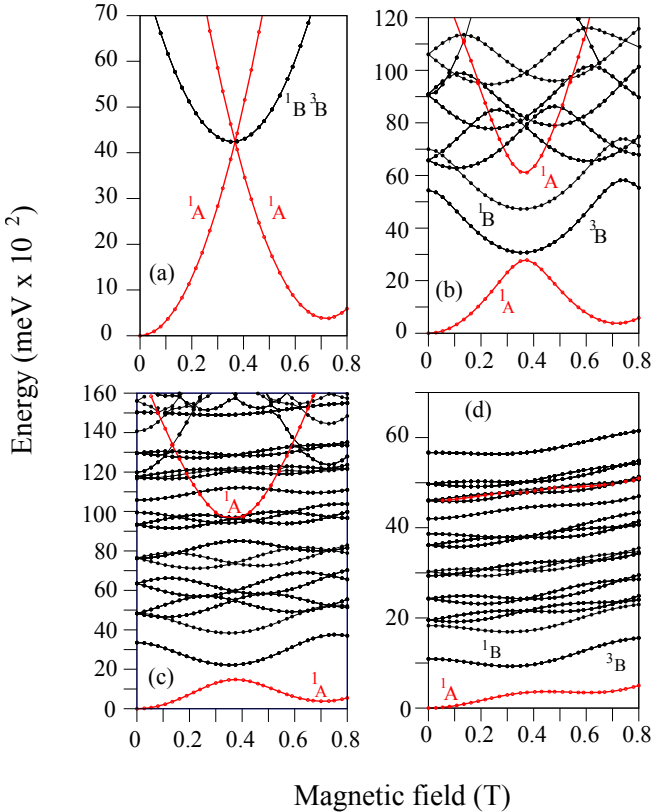


Fig. 4: Lowest-lying states for $N = 6$ for increasing Coulomb interaction. In the panels (a), (b), (c) and (d) the Coulomb repulsion is scaled down by a factor of 0, 0.1, 0.2 and 0.5, respectively. Red lines correspond to the states which anticrossing is responsible of the suppression of the AB effect and of the flat magnetization profile.

observe a neat fractional behaviour only for $N = 2$. As far as the $N = 6$ case is concerned, fig. 5 reveals that the AB suppression is no longer present. This is because in this density regime the magnitude of the anticrossing between the two 1A states of the $N = 6$ system cannot overcome the relative stabilization of the triplet 3B state coming from the exchange integrals (see fig. 4) so that 3B emerges as the ground state in a narrow window around one half of flux, yielding an irregular discontinuity in the magnetization profile around this magnetic field, as reported in fig. 5.

Role of symmetry and conclusions. – To conclude, we explore whether or not the suppression of the AB effect may occur in QRs of symmetries other than C_6 . To this end, we take into account the previous result relating the suppression of the AB effect to the anticrossing between the $B = 0$ ground state and an excited state of the same symmetry and total spin. In particular, the symmetry of the N -electron state can be calculated as the product of the irreps of the orbitals in the leading configuration. Furthermore, the orbital

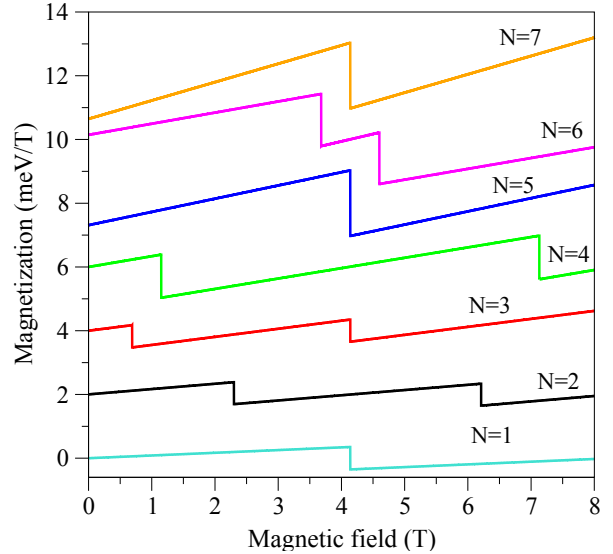


Fig. 5: Magnetization of the small hexagonal QR (three times smaller than in previous figures) for $N = 1$ (bottom) up to $N = 7$ (top). For the sake of clarity, the different magnetization profiles have been offset by 2 meV/T.

ordering can also be determined from that of a circular QR by considering the symmetry reduction $C_\infty \rightarrow C_n$. We give the mathematical details in the Appendix. By considering the C_n symmetry groups with $n = 3$ up to $n = 10$ (i.e. from triangular to decagonal shape) we prove that, besides the $N = 6$ hexagonal QR, the smallest C_n group that may render a possible anticrossing is the $N = 10$ C_{10} -symmetry QR. On the one hand, C_{10} is not a geometry that can be realistically synthesized at the nanometric level, on the other hand, the relatively large number of electrons required, $N = 10$, and the need of a low-density regime points this regime as difficult to be experimentally achieved. Then, we may say that no other ground state anticrossing like that of the $N = 6$ case in hexagonal QRs can occur for the currently synthesized geometries.

In summary, we have shown that hexagonal QRs exhibit AB phenomena different from the well-known circular rings. The most remarkable finding is the complete suppression of the AB effect when the six-electron hexagonal QR system is in the high-correlation, low-density regime. The phenomenon originates in the anticrossing between the $B = 0$ ground state and an excited state of the same symmetry and total spin. We have demonstrated that this effect is exclusive of hexagonal structures and it implies the possibility of switching on and off the device magnetization by varying the number of confined carriers.

Appendix. – A C_n group has n irreps labelled with $k = 0 \pm 1 \pm 2 \dots$ up to the integer part of $n/2$. The $k = 0$ irrep is generally referred to as A and it is real and fully

symmetric. The remaining irreps are complex and labelled E_k^\pm . For even n , $k = n/2$ and $k = -n/2$ correspond to the same real and fully antisymmetric irrep B . The character $\chi_{\pm k}(C_n^m)$ of the irrep k ($-k$) corresponding to an angle $2\pi m/n$ around the rotation axis of the C_n group is:

$$\chi_{\pm k}(C_n^m) = \exp\left[\pm i \frac{2\pi}{n} k m\right] \quad (3)$$

This expression allow us to write the character table of any C_n group. All the same, if $k = np + q$ with $q = 0, 1, \dots, (n-1)$ and $p = 0, 1, 2, \dots$, the following identities,

$$\exp\left[\pm i \frac{2\pi}{n} (np + q) m\right] = \exp\left[\pm i \frac{2\pi}{n} q m\right] \quad (4)$$

$$\exp\left[\mp i \frac{2\pi}{n} (n - q) m\right] = \exp\left[\pm i \frac{2\pi}{n} q m\right] \quad (5)$$

allow us to conclude that:

$$\chi_{\pm k}(C_n^m) = \begin{cases} \chi_{\pm q}(C_n^m); & q \leq k_M \\ \chi_{\mp(n-q)}(C_n^m); & q > k_M \end{cases} \quad (6)$$

where k_M is the integer part of $n/2$, i.e., the largest value of k in the character table of C_n .

The last result allow us to determine the symmetry $C_\infty \rightarrow C_n$ reduction table. Thus, for even n , the C_∞ irreps labelled as $k = 0, 1, -1, 2, -2, \dots$ correspond to $A, E_1^+, E_1^-, E_2^+, E_2^-, \dots, E_{k_M-1}^+, E_{k_M-1}^-, B, B, E_{k_M-1}^-, \dots, E_1^-, E_1^+, A, A, E_1^+, E_1^-, \dots$. For odd n they correspond to $A, E_1^+, E_1^-, \dots, E_{k_M}^+, E_{k_M}^-, E_{k_M}^-, E_{k_M}^+, \dots, E_1^-, E_1^+, A, A, E_1^+, E_1^-, \dots$. This symmetry reduction scheme helps to understand the evolution vs. the magnetic field of the single-particle orbitals of polygonal rings pierced by an axial magnetic field: sets of non-crossing shells containing n orbitals with different symmetry repeatedly crossing as the magnetic field increases (see e.g. fig. 1).

As for the product of irreps we have:

$$\chi_{\pm k_1}(C_n^m) \chi_{\pm k_2}(C_n^m) = \exp\left[i \frac{2\pi}{n} [(\pm k_1) + (\pm k_2)] m\right] \quad (7)$$

Then, the product of two irreps $\pm k_1, \pm k_2$ yields the irrep labelled with the sum $k = (\pm k_1) + (\pm k_2)$. In case the resulting k is larger than k_M , then we write $k = np + q$ with $q < n$ and identify k with q (with $-(n - q)$) if $q \leq k_M$ ($q > k_M$).

With this information we may adress the problem of anticrossings. The scheme of orbital energies vs. the magnetic field is shown in fig. 6.

In order to have, at a given value of the magnetic field, an anticrossing between two N -electron states that are the ground state in either side of the avoided crossing, the dominant electronic configuration in either side of the

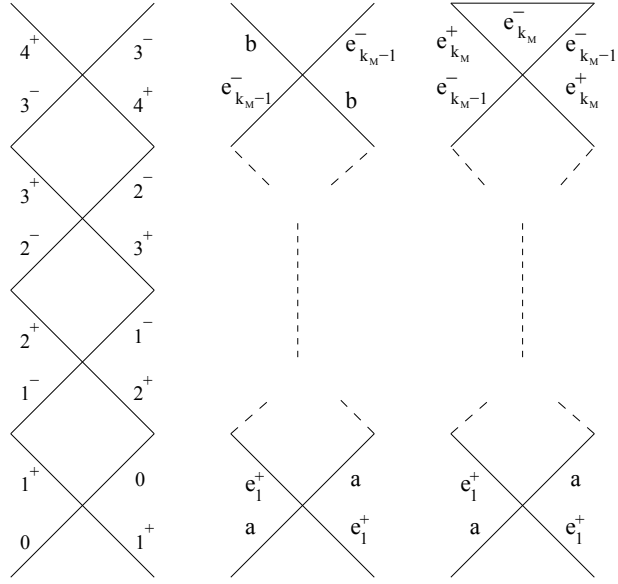


Fig. 6: Scheme of the orbital energies vs. the magnetic field. Left: low-lying part of the energy spectrum corresponding to a C_n symmetry with large n . The orbitals are labelled by $k = 0 \pm 1 \pm 2 \pm 3 \dots$. Center: top and bottom of the orbital shell for even n . The notation for orbitals, $\{A, e_k^\pm (k = 1, 2 \dots k_{M-1}), B\}$, is that of the C_n irreps. Right: top and bottom of the orbital shell for odd n . The C_n notation $\{A, e_k^\pm (k = 1, 2 \dots k_M)\}$ is used.

monoelectronic crossing must be different yet it must yield the same symmetry and total spin for the N -electron state. This cannot occur for odd number N of electrons. For even N it can only occur if the square of the irreps Γ_{-k} and Γ_{k+1} , $k + 1 \leq k_M$ yield the same irrep, i.e., if

$$\chi_{-k}(C_n^m)^2 = \chi_{k+1}(C_n^m)^2 \quad (8)$$

with

$$\chi_{-k}(C_n^m)^2 = \exp\left[-i \frac{4\pi}{n} k m\right] \quad (9)$$

$$\chi_{k+1}(C_n^m)^2 = \exp\left[i \frac{4\pi}{n} (k+1) m\right] \quad (10)$$

It obviously occurs for $m = 0$. It must be also true for $m = 1, 2, 3 \dots (n-1)$, i.e., it must occur both that q be a natural number ($q \in N$) and the fulfilment of the identity:

$$\frac{4\pi}{n} (k+1) m = 2\pi q - \frac{4\pi}{n} k n \quad (11)$$

In other words,

$$k = \frac{1}{4} \left(\frac{nq}{m} - 2 \right), \quad m = 1, 2, \dots, (n-1) \quad \text{and} \quad q \in N \quad (12)$$

It obviously holds for $(k = 1, n = 6)$, for we may just select $q = m$ in eq. 12. It cannot hold for $n = 3$. In this case we have three irreps $k = 0 \pm 1$. Then, $q = (2k+2)m/n$

must be a natural number for $k = 0, m = 0, 1$, which is not the case ($q = 2m/3 \notin N$ for $m = 0, 1$). In Table 1 we enclose the possible q values for the symmetry groups C_n from $n = 3$ up to $n = 10$ as a function of m . Since for a given group C_n the irrep label k_M is equal to the integer part of $n/2$, we have then a single possible k for C_3 , two of them for C_4 and C_5 , three for C_6 and C_7 , etc.

Table 1: Possible q values for the symmetry groups C_n from $n = 3$ up to $n = 10$ as a function of $m = 1, 2, \dots, (n - 1)$. The integer values are highlighted.

$n \backslash k$	0	1	2	3	4
3	m				
4	m	$\frac{3}{2}m$			
5	m	$\frac{5}{2}m$			
6	m	m	$\frac{5}{3}m$		
7	m	$\frac{6}{5}m$	$\frac{10}{7}m$		
8	m	$\frac{7}{3}m$	$\frac{4}{5}m$	$\frac{7}{4}m$	
9	m	$\frac{8}{5}m$	$\frac{10}{9}m$	$\frac{14}{7}m$	
10	m	m	m	$\frac{9}{5}m$	$\frac{9}{5}m$

As we can see in Table 1, up to the symmetry group C_{10} , no ground state anticrossing occurs except for ($n = 6, k = 1$) and ($n = 10, k = 2$). In other words, for the currently synthesized geometries, only the hexagonal one presents the ground state anticrossing when the number of electron just fills the e_2^+ with two electrons. As discussed in previous sections, this anticrossing has deep physical consequences if the system is the high correlation low-density regime.

This work was partially supported by UJI-Bancaixa Project No. P1-1B2011-01, MCINN Project No. CTQ2011-27324, and FPI and FPU Grants (A.Ba. and C.S.). A.Be. acknowledges the CINECA award under the ISCRa initiative for high performance computing resources.

REFERENCES

- [1] Noborisaka J., Motohisa J., Hara S. and Fuku T., *Appl. Phys. Lett.* **87** (2005) 093109.
- [2] Fontcuberta i Morral A., Spirkoska D., Arbiol J., Heigoldt M., Morante J. R. and Abstreiter G., *Small* **4** (2008) 899.
- [3] Algra R. E., Hocevar M., Verheijen M. A., Zardo I., Immink G. G. W., van Enckevort W. J. P., Abstreiter G., Kouwenhoven L. P., Vlieg E. and Bakkers E. P. A. M., *Nano Letters* **11** (2011) 1690.
- [4] Keplinger T. M. M., Stangl J., Wintersberger E., Mandl B., Kriegner D., Hol V., Bauer G., Deppert K. and Samuelson L., *Nano Letters* **9** (2009) 1877.
- [5] Rudolph D., Funk S., Döblinger M., Morkötter S., Hertenberger S., Schweickert L., Becker J., Matich S., Bichler M., Spirkoska D., Zardo I., Finley J.J., Abstreite G. and Koblmüller G., *Nano Letters* **13** (2013) 1522.
- [6] Royo M., Bertoni A. and Goldoni G., *Phys. Rev. B* **87** (2013) 115316.
- [7] Lauhon L. J., Gudiksen M. S., Wang D. and Lieber C. M., *Nature* **420** (2002) 57.
- [8] Shen G., Chen D., Bando Y. and Golberg D., *J. Mater. Sci. Technol.* **24** (2008) 541.
- [9] Shen G. and Chen D., *Sci. Adv. Mater.* **1** (2009) 353.
- [10] Heigoldt M., Arbiol J., Spirkoska D., Rebled J. M., Conesa-Boj S., Abstreiter G., Peir F., Morante J. R. and Fontcuberta i Morral A. *J. Mater. Chem.* **19** (2009) 840.
- [11] Hasen J., Pfeiffer L. N., Pinczuk A., He S., West K.W. and Dennis B.S., *Nature* **390** (1997) 54; Fasth C., Fuhrer A., Björk M. T. and Samuelson L., *NanoLett.* **5** (2005) 1487; Tatebayashi J., Ota Y., Ishida S., Nishioka M., Iwamoto S. and Arakawa Y., *Appl. Phys. Lett.* **100** (2012) 263101.
- [12] Fuhrer A., Lscher S., Ihn T., Heinzl T., Ensslin K., Wegscheider W. and Bichler M., *Nature* **413** (2001) 822.
- [13] Lorke A., Luyken R. J., Govorov A. O., Kotthaus J., García J. M., and Petroff P. M., *Phys. Rev. Lett.* **84** (2000) 2223.
- [14] Viefers S., Koskinen P., Deo P. S. and Manninen M., *Physica E* **21** (2004) 1.
- [15] Filikhin I., Suslov V. M. and Vlahovic B., *Physica E* **33** (2006) 349.
- [16] Chakraborty T. and Pietilainen P., *Phys. Rev. B* **50** (1994) 8460.
- [17] Barticevic Z., Pacheco M. and Latg A., *Phys. Rev. B* **62** (2000) 6963.
- [18] Climente J.I., Planelles J. and Jaskolski W., *Phys. Rev. B* **68** (2003) 075307; Climente J.I., Planelles J. and Movilla J. L., *Phys. Rev. B* **70** (2004) 081301.
- [19] Ballester A., Planelles J. and Bertoni A., *J. Appl. Phys.* **112** (2012) 104317.
- [20] Lipparini L. E., *Modern Many-Particle Physics*, (World Scientific, Singapore) 2008.
- [21] Keyser U. F., Fühner C., Borck S., Haug R. J., Bichler M., Abstreiter G. and Wegscheider W., *Phys. Rev. Lett.* **90** (2003) 196601.
- [22] Emperador A., Pederiva F. and Lipparini E., *Phys. Rev. B* **68** (2003) 115312.
- [23] Niemelä K., Pietiläinen P., Hyvönen P. and Chakraborty T., *Europhys. Lett.* **36** (1996) 533.
- [24] Liu Y. M., Huang G. M. and Shi T. Y., *Phys. Rev. B* **77** (2008) 115311.
- [25] Kusmartsev F. V., Weisz J. F., Kishore R. and Takahashi M., *Phys. Rev. B* **49** (1994) 16234.